Molecular Biology of the Cell
Vol. 17, 1204–1217, March 2006

Deregulation of HEF1 Impairs M-Phase Progression by Disrupting the RhoA Activation Cycle

Disha Dadke,* Michael Jarnik, Elena N. Pugacheva, Mahendra K. Singh, and Erica A. Golemis

Division of Basic Science, Fox Chase Cancer Center, Philadelphia, PA 19111

Submitted March 21, 2005; Revised December 18, 2005; Accepted December 28, 2005
Monitoring Editor: Jean Schwarzbauer

The focal adhesion-associated signaling protein HEF1 undergoes a striking relocalization to the spindle at mitosis, but a function for HEF1 in mitotic signaling has not been demonstrated. We here report that overexpression of HEF1 leads to failure of cells to progress through cytokinesis, whereas depletion of HEF1 by small interfering RNA (siRNA) leads to defects earlier in M phase before cleavage furrow formation. These defects can be explained mechanistically by our determination that HEF1 regulates the activation cycle of RhoA. Inactivation of RhoA has long been known to be required for cytokinesis, whereas it has recently been determined that activation of RhoA at the entry to M phase is required for cellular rounding. We find that increased HEF1 sustains RhoA activation, whereas depleted HEF1 by siRNA reduces RhoA activation. Furthermore, we demonstrate that chemical inhibition of RhoA is sufficient to reverse HEF1-dependent cellular arrest at cytokinesis. Finally, we demonstrate that HEF1 associates with the RhoA-GTP exchange factor ECT2, an orthologue of the *Drosophila* cytokinetic regulator Pebble, providing a direct means for HEF1 control of RhoA. We conclude that HEF1 is a novel component of the cell division control machinery and that HEF1 activity impacts division as well as cell attachment signaling events.

INTRODUCTION

As points of structural linkage between the extracellular matrix (ECM) and the intracellular cytoskeleton, focal adhesions possess a complex function. For example, during migration, cells must rapidly break down and reform adhesions with the ECM, providing force for propulsion (Lauffenburger and Horwitz, 1996). At mitotic entry, cultured cells round up and decrease adhesion to the ECM; at mitotic exit, basal attachments reassemble and contribute to the force generation required for efficient progress through cytokinesis and reentry into G_1. In interphase cells, the formation of novel focal adhesion–ECM interactions can specify cellular differentiation by activating specific signaling cascades culminating in the induction of differentiation-promoting transcription factors, and in parallel enforce removal from the cell cycle (Boudreau and Bissell, 1998). In many cell types, sustained loss of adhesion is a sufficient stimulus to induce apoptosis (anoikis) (Frisch and Francis, 1994), a surveillance mechanism against cancer, inhibiting the formation of micrometastases. Hence, one frequent effect of oncogenic transformation is the circumvention of the adhesion–viability coupling, leading to acquisition by cancer cells of the ability to grow in an anchorage-independent manner (Schwartz, 1997). Based on these diverse biological roles, there has been considerable research effort directed at elucidating the signaling role of focal adhesion-associated proteins (Schlaepfer *et al*., 1999).

HEF1, p130Cas, and Efs/Sin define the Cas family of proteins (O'Neill *et al*., 2000; Bouton *et al*., 2001). In interphase cells, Cas proteins predominantly localize to focal adhesions. During initial integrin engagement, induced by cell attachment to the extracellular matrix, Cas proteins are phosphorylated by focal adhesion kinase (FAK) (Polte and Hanks, 1995; Law *et al*., 1996) and subsequently targeted by Src family kinases (Sakai *et al*., 1994; Inoue *et al*., 1995; Ishino *et al*., 1995; Alexandropoulos and Baltimore, 1996; Nakamoto *et al*., 1996; Vuori *et al*., 1996; Sakai *et al*., 1997). The result of Cas–FAK–Src interactions is extensive tyrosine phosphorylation of Cas proteins, nucleating formation of complexes with adaptor proteins including CrkII, C3G, and DOCK180, providing both prosurvival and promotility signaling: these well studied Cas activities are beyond the scope of this study.

It has long been known that loss of cell adhesion can cause mitotic defects, most notably by causing failure of cytokinesis (Orly and Sato, 1979; Ben-Ze'ev and Raz, 1981), potentially through loss of traction forces that cells use to physically separate. However, because adhesion is most readily observable in interphase cells, and focal adhesions tend to minimize or disappear in mitotic cells, accompanied by the down-regulation of some key focal adhesion-associated signaling proteins (Yamaguchi *et al*., 1997; Law *et al*., 1998; Yamakita *et al*., 1999), little work has investigated a possible requirement or alternative roles for adhesion-associated proteins in M phase. Similarly, it is only in the past several years that investigations of the nuclear cell cycle have documented the coordination of signaling events in time and space during M-phase progression, emphasizing the roles of proteins associated with structures such as the centrosome, the contractile ring, the central spindle, and the midbody (Raff *et al*.,

This article was published online ahead of print in *MBC in Press* (http://www.molbiolcell.org/cgi/doi/10.1091/mbc.E05–03–0237) on January 4, 2006.

* Present address: Stem Cell Research Center, Manipal Hospital, Bangalore 560017, India.

Address correspondence to: Erica Golemis (ea_golemis@fccc.edu) or Disha Dadke (disha.dadke@manipalhospital.org).

2002; reviewed in Glotzer, 2001). An economical view of cellular function would suggest that the reuse of proteins that govern cell adhesion and cytoskeletal dynamics in interphase cells might provide an efficient means to synchronize changes in cell contacts during mitosis.

Indeed, recent studies have emphasized the importance of cytoskeletal regulatory factors such as the RhoA GTPase not only in control of stress fibers and cell migration in interphase cells (Ridley and Hall, 1992; Ridley, 2001) but also in regulating cortical actin dynamics in mitosis and cytokinesis (Glotzer, 2001; Maddox and Burridge, 2003). Furthermore, a number of proteins most studied in the context of action at focal adhesions, including zyxin (Hirota *et al*., 2000), paxillin (Yamaguchi *et al*., 1997), FAK (Yamakita *et al*., 1999; Fresu *et al*., 2001; Ma *et al*., 2001), and the Cas family member HEF1 (Law *et al*., 1998), have been implicated in mitotic control, based on dramatic changes in their phosphorylation, or their localization to mitotic structures, in M phase. We have begun to investigate the role of HEF1 as a direct regulator of mitotic progression, and through this work, we have recently demonstrated that HEF1 associates with and positively regulates the Aurora-A kinase at mitotic entry (Pugacheva and Golemis, 2005). We also showed that overexpression of HEF1, like hyperactivation of Aurora-A, promotes supernumerary centrosomes and multipolar spindles, but these phenotypes are not seen in HEF1-induced cells that have been held in S phase, suggesting they are secondary to an initial defect in transition through mitosis. We here investigate the consequences of either overexpressing or depleting HEF1 for mitotic progression. Based on this work, we conclude that HEF1 has important roles in specifying mitotic rounding, cleavage furrow ingression, and cytokinesis and that HEF1 accomplishes these roles based on its ability to regulate the activation cycle of RhoA during M phase, potentially through interaction with the RhoA activator ECT2.

MATERIALS AND METHODS

Cell Lines and Materials

MCF-7 human breast carcinoma cells were cultured in DMEM supplemented with 10% fetal bovine serum (FBS), 50 U ml^{-1} penicillin, and 50 μg ml^{-1} streptomycin. The construction of MCF-7 transfectants carrying either full-length HEF1, or empty vector under the control of a tetracycline-repressible operator, and procedures for HEF1 induction, have been described previously (Fashena *et al*., 2002). The plasmids pCDNA-HEF1, pCatchFlag-HEF1, and pEGFP-HEF1, encoding full-length HEF1 used for transient expression of HEF1, have been described previously (Law *et al*., 1998). Note that HEF1 has been assigned the symbol NEDD9 by The International Radiation Hybrid Mapping Consortium. The vectors pCMV6HA, pCatchFlag, and pEGFP-C4 (Clontech, Mountain View, CA) were used as a control for transient transfection assays. pCMV6M-RhoL63, expressing constitutively active RhoA, was a kind gift from Dr. Chernoff (Fox Chase Cancer Center, Philadelphia, PA). pCEV29F3-ECT2 was generously provided by Dr. Miki (National Cancer Institute, Bethesda, MD) and later modified by subcloning into pCMV6HA plasmid. The anti-HEF1 rabbit polyclonal antibody (Law *et al*., 1998) and HEF1 monoclonal antibodies (Pugacheva and Golemis, 2005) have been described previously. Other antibodies used include anti-RhoA monoclonal antibody (mAb) and anti-p130Cas mAb from BD Biosciences (San Jose, CA); anti-α-tubulin (clone DM 1A) and anti-myosin light chain (MLC) mAb from Sigma-Aldrich (St. Louis, MO); anti-ECT2 (C-20 and H-300), anti-p160ROCK, anti-phospho-MLC polyclonal antibody, anti-hemagglutinin (HA), and anti-Flag mAbs from Santa Cruz Biotechnology (Santa Cruz, CA); anti-green fluorescent protein (GFP) mAb and clone JL-8 from BD Biosciences (San Jose, CA); anti-Cyclin B1 mAb from BD Biosciences PharMingen (San Diego, CA); and rhodamine-conjugated anti-mouse and anti-rabbit antibodies, Alexa Fluor488-conjugated anti-mouse antibodies, and fluorescein isothiocyanate (FITC)-conjugated phalloidin (Molecular Probes, Eugene, OR). C3 transferase protein was from Cytoskeleton (Denver, CO), and Y-27632 was from EMD Biosciences (San Diego, CA). Glutathione *S*-transferase (GST)-fused Rhotekin Rho binding domain (RBD), agarose Histone H2B, and anti-phospho-Histone H2B were from Upstate Biotechnology (Lake Placid, NY). Pansorbin cells were from Calbiochem (San Diego, CA).

Cell Culture

MCF-7 cells expressing empty vector control or full-length HEF1 from a tetracycline-repressible promoter were maintained in DMEM supplemented with FBS, 50 U ml^{-1} penicillin, 50 μg ml^{-1} streptomycin, 400 μg ml^{-1} puromycin, and 1 μg ml^{-1} tetracycline. Where indicated, MCF-7 cells were transfected using LipofectAMINE Plus reagent (Invitrogen, Carlsbad, CA) according to the manufacturer's protocol. Tumor necrosis factor (TNF)-α treatment of stable cell lines was carried out by plating cells directly into fresh DMEM plus 10% FBS, with or without addition of tetracycline as indicated, containing 100 ng ml^{-1} TNF-α. Blockade of caspase-3 and -7 activation was accomplished by incubation with cell-permeating caspase inhibitor z-DEVD-fmk at a final concentration of 25 μM.

Small Interfering RNA (siRNA) Transfection

To design target-specific siRNA duplexes, we selected sequences of the type $AA(N_{19})$, where N is any nucleotide, from the open reading frame of HEF1 gene sequence (accession no. NM-006403). The selected sequence was also submitted to a BLAST search against the human genome sequence to ensure that only the HEF1 gene of the human genome was targeted. The siRNA sequence targeting HEF1 was from position 737–757 relative to the start codon. An siRNA duplex against the selected HEF1 sequence, a nonspecific scrambled oligonucleotide (oligo) siRNA and an siRNA duplex against ECT2 (ECT2 NM-018098) were made by Dharmacon Research, (Lafayette, CO). Transient transfection of siRNAs was carried out using OligofectAMINE (Invitrogen). Cells were assayed after 48 h of transfection. For each experiment, specific silencing was confirmed by Western blotting and by immunofluorescence. To synchronize cells in G_2/M phase, 44 h post-siRNA transfection cells were blocked with 2 μM nocodazole for 4 h. Cells were then harvested by mitotic shake-off and analyzed by flow cytometry and Western blotting. To synchronize cells in G_1/S phase, cells were transfected with siRNA and 12 h posttransfection, cells were blocked with double thymidine, released, and analyzed by flow cytometry and Western blotting. To estimate the percentage of round mitotic cells after siRNA treatment, cells were also tracked for 12 h under a phase contrast microscope at 20× magnification after release from double thymidine, to score for the appearance of round mitotic cells. To quantitate data for HEF1 depletion or induction, for Western analysis, densitometric analysis of the enhanced chemiluminescence-exposed blots was done using the NIH ImageJ (version 1.24o) software. Briefly, a Western blot is exposed to film, and the film is scanned. Next, the program NIH Image is used to draw a box around the lanes corresponding to each of the protein bands being quantified, whereas a box of identical side is drawn around a nearby empty lane. The program calculates the signal intensity of the specific band minus the background (empty lane), allowing a rough estimate of intensity differences. The typical range of depletion is 80–90% (working with less exposed gels to avoid signal saturation for the controls), with outlying values of 75–95%. For some experiments, titration of control depleted versus HEF1-depleted extracts was also done.

Videomicroscopy and Image Processing

MCF-7 cells expressing HEF1 either transiently or stably, or transiently transfected with pCMV6M-RhoL63, transfected with siRNAs were maintained at 37°C in a stage incubator built on top of an Nikon Eclipse E800 inverted microscope fitted with Ludl X, Y and Z controllers, a five-position filter wheel, and a uniblitz shutter (Carl Zeiss, Thornwood, NY) and viewed with a 20× numerical aperture Plan Fluor lens. All images were acquired with a Quantix cooled charge-coupled device (CCD) camera (Roper Scientific, Trenton, NJ) and the ISee imaging program (ISee Imaging Systems, Raleigh, NC).

Immunofluorescence Studies

Asynchronous cells, or cells synchronized by double thymidine or nocodazole block, were cultured on coverslips, fixed in 4% paraformaldehyde (EM Scientific, Gibbstown, NJ), permeabilized in 0.5% Triton X-100 for 5 min, and blocked with 3% bovine serum albumin in phosphate-buffered saline. After incubation with primary antibodies, the cells were stained with rhodamine X-conjugated anti-rabbit antibodies along with Alexa Fluor 488-conjugated anti-mouse antibodies. For staining of filamentous actin, FITC-conjugated phalloidin was included during incubation with the secondary antibodies. Confocal microscopy was performed using a Radiance 2000 laser scanning confocal microscope (Bio-Rad, Hercules, CA) coupled to a Nikon Eclipse E800 upright microscope (Carl Zeiss). All optical sectioning was carried out in 0.5-μm increments.

Electron Microscopy

The cells were fixed by the method of Maupin and Pollard (1986)). Briefly, the cells were fixed using glutaraldehyde-tannic acid-saponin and then osmium, and serial sections were prepared. Micrographs were taken on a FEI Technai 12 electron microscope operated at 80 kV using an AMT 2kx2k CCD camera.

Cell Cycle Synchronization for HEF1 Stable Cell Lines

Cells were synchronized at G_1/S phase by double thymidine block (Cos *et al*., 1996). Cells thus synchronized were then cultured in fresh DMEM containing 10% FBS and 1 μg ml^{-1} tetracycline. After 5 h, nocodazole or taxol was added at final concentration of 1 or 0.1 μM, respectively, in the presence or absence of tetracycline for another 7 h to collect G_2/M phase cells overexpressing HEF1. Round mitotic cells were further purified by shake-off. Collected cells were suspended in fresh DMEM containing 10% FBS with or without tetracycline at release from the nocodazole or taxol arrest. At 0, 30, 60, and 90 min after the release, cells were harvested and analyzed. To study the effect of HEF1 overexpression on G_1/S phase, cells were blocked with double thymidine as described above except for concurrent induction of HEF1 expression for last 6 h of the second thymidine block by removal of tetracycline. Flow cytometry analysis was done using FACSII instrument (BD Biosciences, Franklin Lakes, NJ). For Western blot analysis, samples were resolved by a 7.5% SDS-PAGE, transferred to Immobilon-P membranes (Millipore, Billerica, MA), analyzed by immunoblotting using relevant antibodies, and results were quantitated as described above for Western analysis. Cyclin B1 levels were quantitated by running the cell lysates on 10% SDS-PAGE and probing with anti-Cyclin B1 antibody. Subsequently, blots were stripped and reprobed with anti-β-actin antibody to confirm equal loading.

Pull-Down Assays for GTP-RhoA

Cells were lysed in PTY buffer containing 1× protease inhibitors (Roche Diagnostics, Mannheim, Germany) and phosphatase inhibitor cocktails I and II (Sigma-Aldrich). Then, 500 μg of cell lysate was incubated with 25 μg of GST-RBD fusion conjugated with agarose beads at 4°C for 2 h. The beads were washed twice with lysis buffer and subjected to SDS-PAGE on a 4–20% gel. Bound RhoA was detected by Western blot using monoclonal α-RhoA, and results were quantitated as described above.

p160ROCK and Phospho-MLC Assays

p160ROCK kinase activity was assayed by lysing cells in PTY lysis buffer and preclearing the lysates (250 μg) by incubating them with 20 μl of Pansorbin cells for 20 min at 4°C. p160ROCK was immunoprecipitated by incubating with 3 μg of anti-p160ROCK antibody per sample at 4°C, O/N, followed by pull-down with protein A-Sepharose at 4°C for 60 min. After washing two times with lysis buffer and two times with kinase buffer (50 mM Tris, pH 7.4, 100 mM NaCl, 10% glycerol, 0.05% Triton-X, 2 mM $MgCl_2$, 2 mM $MnCl_2$, 1 mm Na_3VO_4, and 10 mM NaF), immunoprecipitates were incubated with 1 μg of Histone H2B in reaction buffer (kinase buffer plus 10 μM ATP) for 30 min at 37°C. Phosphorylation reactions were stopped by addition of Laemmli buffer, resolved by 10% SDS-PAGE, and probed with anti-phospho-Histone H2B antibody. Total p160ROCK in whole cell lysates was established by direct Western analysis with p160ROCK antibody. To quantitate the p160ROCK activity, the immunoprecipitations (IP) and direct Western blots were analyzed by NIH ImageJ analysis software, and individual phospho-Histone H2B values were normalized to total p160ROCK values. Quantitation of phosphorylation of MLC was performed by running whole cell lysates on 10% SDS-PAGE, blotting and probing first with phospho-specific antibody against MLC, followed by stripping the blot in stripping buffer (Pierce Chemical, Rockford, IL) and then probing with anti-MLC antibody. To quantitate the levels of phosphorylated MLC, these blots were analyzed by NIH ImageJ analysis software and phospho-MLC, levels were obtained by normalizing phospho-MLC values to total MLC values.

Immunoprecipitation

For HEF1and ECT2 immunoprecipitation, cells were cotransfected with empty vectors alone (pCMV6HA and pCatchFlag or pCMV6HA and pEGFP) or vector alone with vector expressing appropriate tagged protein (pCMV6HA and pEGFP-HEF1 or pCMV6HA-ECT2 and pEGFP or pCMV6HA and pCatchFlag-HEF1 or pCatchFlag and pCMV6HA-ECT2) or vectors expressing different tagged proteins together (pCMV6HA-ECT2 and pEGFP-HEF1 or pCMV6HA-ECT2 and pCatchFlag-HEF1). Note that different combinations of tagging constructs were used to reduce the possibility of artifactual enhancement or inhibition of coimmunoprecipitation based on the nature of the attached epitope tag. Cells were lysed in M-PER Mammalian protein extraction reagent (Pierce Chemical) and immunoprecipitated with either anti-HA or anti-Flag mAbs using protein A/G-Sepharose (Invitrogen). Precipitates were subjected to 7.5% SDS-PAGE, transferred as described above. Blots were probed with antibodies as indicated in figure legends.

Inhibition of RhoA Activation and p160ROCK Kinase Activity

HEF1.M1 cells were synchronized as described above. Three hours postnocodazole release, HEF1.M1 cells cultured without tetracycline were treated with C3 transferase protein (34 μg ml^{-1}) or Y-27632 (3 μM) as described in Arthur and Burridge (2001) for 30 and 10 min, respectively. Cells were collected and analyzed by flow cytometry. Phase contrast images were collected with a Nikon phase contrast 2 microscope (Carl Zeiss), Pixera Pro150ES camera (Nyoptics, Danville, CA), and Micrografx Picture Publisher 10 software (Corel, Dallas, TX).

RESULTS

Overexpression of HEF1 Causes Failure of Abscission at the End of Mitosis

To determine whether HEF1 has an important function in mitosis, we examined entry into and progression through mitosis in cell lines created in MCF-7 cells with HEF1 (HEF1.M1 and HEF1.M2) or vector (CM1) under control of a tetracycline-repressible promoter (Figure 1A). Cells were observed by time-lapse videomicroscopy to score individual cells passing through mitosis (Figure 1B). Cells with induced HEF1 expression had a significantly increased number of cells that failed to complete cytokinesis effectively, with this defect observed in 37–56% of cells initiating mitosis. Three distinct phenotypes were noted in cells with elevated HEF1 levels (Figure 1B and Table 1). In one phenotype (Figure 1B, ii and Table 1, column 1), initial formation of a cleavage furrow is followed by furrow regression, and formation of binucleate cells. In a second phenotype (Figure 1B, iii and Table 1, column 2), mitosis proceeds normally until late telophase, with two rounded cells at the point of abscission; these cells then experience a delay of between 1 and 3 h before reattaching and separating. For these cells, measurement of the time required for progression through different stages of mitosis indicated that the HEF1-overexpressing HEF1. M1 and HEF1. M2 cell lines move through cleavage furrow and midbody formation at the same rate as the control cells, CM1 and HEF1.M1(+Tet). However, after formation of the midbody, induced HEF1.M1 and HEF1.M2 cells did not undergo abscission for 1–3 h compared with control cells, which completed abscission in ~30 min (Figure 1C). A third phenotype (Figure 1B, iv and Table 1, column 3) differs from the second only in that abscission and cell separation completely fail to occur in >11 h of observation: these cells remain as two clearly attached, rounded cells.

To exclude the possibility that HEF1 overexpression defects in M phase might be a secondary consequence of signaling disruption earlier in the cell cycle, HEF1.M1 cells were synchronized in S phase by double thymidine block in the presence of tetracycline (HEF1 repressed); released for 5 h into medium with tetracycline; and then cultured for 7 h with nocodazole, in the presence or absence of tetracycline. Paralleling our previous findings (Fashena *et al*., 2002), HEF1 accumulation became significant at ~7 h after induction (our unpublished data), accompanying cellular accumulation at G_2/M (Figure 1D, +T and −T, 0 h). Three hours after release of these cells from nocodazole, many more HEF1-induced cells remained accumulated in cytokinesis, based on direct observation (our unpublished data) and reflected by an increased number of cells retaining a 4N DNA content (Figure 1D, compare +T and −T). Quantitation of the cytokinetic phenotypes of these cells [Table 1, HEF1.M1(syn)] indicated a comparable or higher level of block at abscission as seen with unsynchronized populations. Separately, we confirmed that the HEF1 induced in these synchronized cells localized as did endogenous HEF1 to the mitotic spindle and that the spindles seemed normal (Figure 1E). These results indicated overexpression of HEF1 beginning in late G_2 was sufficient to induce the mitotic phenotypes.

Finally, because HEF1 and its close family members p130Cas and Efs/Sin are important mediators of signaling related to cell survival (O'Neill *et al*., 2000), we wanted to exclude the possibility that the mitotic consequences of HEF1 deregulation derived in part from a proapoptotic ac-

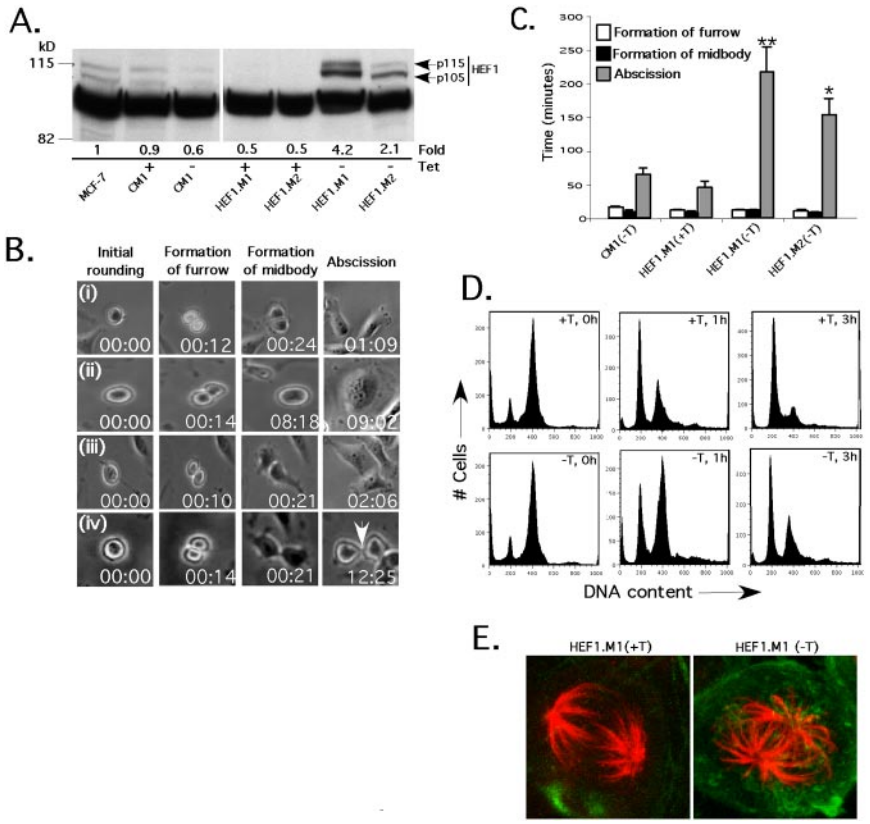

Figure 1. HEF1 overexpression delays mitotic progression and induces abscission defects. (A) Induced expression of HEF1. Western blot analysis of HEF1 expression in stable MCF-7 cells expressing empty vector (CM1) or HEF1 (HEF1.M1 and HEF1.M2) from a tetracycline-repressed promoter in the presence (+T) and absence (−T) of tetracycline, 24 h after induction; quantitation reflects fold-expression relative to MCF-7 cells. Typically, the cell lines maintained with tetracycline present have levels of HEF1 reduced versus the MCF-7 parental line. Note, HEF1 occurs as a doublet migrating at 105 and 115 kDa, reflecting differentially phosphorylated forms. Details of this phosphorylation and antibody characterization have been published in Law *et al*. (1996). (B) Timing of progression through M phase and M-phase defects induced by HEF1 overexpression. (i) Events occurring during normal M-phase progression, time denoted in hours:minutes after initial cell rounding. Cleavage furrow formation and ingression is evident at ~00:12, formation of midbody at ~00:24, and abscission and cell separation complete at 1:09. Three different phenotypes observed on overexpression of HEF1 include (ii) cleavage furrow regression and formation of a binucleate cell (seen at 8:18), (iii) delay between formation of a midbody structure and abscission, and (iv) failure to undergo abscission and cell separation within the period of observation (>12 h). In this last case, daughter cells remain joined by a postmitotic bridge (white arrow). (C) Time required for each stage of M phase, calculated for 15 cells for each sample in three different experiments, using solely cells that had been shown to ultimately undergo separation (e.g., corresponding to the Figure 1B, iii phenotype described above). Results are expressed in minutes ± SE of mean required for formation of cleavage furrow after initial rounding of cell, time from cleavage furrow to formation of a midbody, and time from midbody formation to final abscission. *$p < 0.001$ and **$p < 0.05$. (D) HEF1 overexpression inhibits progress of cells through M phase. HEF1.M1 cells cultured in medium with tetracycline were synchronized at S phase with a double thymidine block, released for 5 h, blocked with nocodazole for 7 h in the presence or absence of tetracycline to induce HEF1 expression, and collected by mitotic shake-off. After nocodazole release, cells were followed for 3 h. Within panels, +/−T, with/without tetracycline; 0 h, 1 h, and 3 h, time after release from nocodazole. (E) Mitotic spindles of HEF1.M1 cells in the presence (+T) or absence (−T) of tetracycline. HEF1 is shown in red; actin in green.

tivity (discussed in Law *et al*., 2000; O'Neill and Golemis, 2001). The observed effect of enhanced HEF1 levels on cytokinesis is not a secondary consequence of apoptosis, based on two criteria: 1) treatment of induced HEF1.M1 cells with the caspase inhibitor z-DEVD-fmk inhibits apoptosis, but it does not reduce the level of cytokinetic defect as assessed by time lapse (Table 2); and 2) treatment of either controls or induced HEF1.M1 cells with TNF-α induces apoptosis, but it does not induce cytokinetic defects as assessed by time lapse (Table 2), thereby indicating that HEF1 induced apoptosis and cytokinetic defects are separate issues. Based on this and the above-mentioned results, we conclude that HEF1 promotes failure of abscission as the result of a direct function exerted in the G_2 and/or M phases of cell cycle.

Reduced HEF1 Levels Cause Defects in Mitotic Entry and Cleavage Furrow Ingression

HEF1 depletion also leads to mitotic timing defects, but at a different stage in M phase than observed with overexpression. HEF1 depletion in MCF-7 cells using targeted siRNAs results in efficient reduction of the protein at 48 h after transfection (Figure 2A). HEF1 depletion did not significantly affect the apoptotic index of treated cells (no nuclei condensation observed by 4,6-diamidino-2-phenylindole staining, no poly(ADP-ribose) polymerase cleavage product

Table 1. M-phase defects accompanying HEF1 overexpression

Cell line	Cleavage furrow regression (%)	Delayed abscission[a] (%)	No abscission (%)
Control			
CM1(−T)	1.2	0	0
HEF1.M1(+T)	0	0	0
HEF1 expressors			
HEF1.M1(−T)	14	20	22
HEF1.M2(−T)	11	11	15
HEF1.M1(syn)	5	4	33

MCF-7-based cell lines with empty vector (CM1) or HEF1 (HEF1.M1, MEF1.M2) from a tetracycline repressible promoter in the presence (+T) and absence (−T) of tetracycline, and HEF1.M1 cells synchronized in S phase with a double thymidine block and released into tetracycline minus medium (syn) also were assessed. Cytokinetic defects characterized by cleavage furrow regression, delayed abscission, or no abscission are indicated. The mitotic fate for 150 cells was determined for each sample in three different experiments.

[a] Delayed abscission describes a situation in which abscission and visible cell separation occurred within 2–3 h; in contrast to no abscission, in which cells remained joined for the period of observation (>12 h).

Table 2. Separation of HEF1-dependent mitotic phenotypes from incidence of apoptosis

Cell lines, treatment	Cleavage furrow regression (%)	Delayed abscission (%)	No abscission (%)	Apoptosis (%)
CM1(−T)	1.2	0	0	7
CM1(−T) + TNF-α	0	0	0	46
HEF1.M1(−T)	14	20	22	33
HEF1.M1(−T) + TNF-α	9	16	26	58
HEF1.M1(−T) + z-DEVD	12	20	24	8

Control (CM1) or HEF1-induced (HEF1.M1) cells were either treated with TNF-α (to induce apoptosis), with z-DEVD-fmk (to inhibit apoptosis), or mock treated. They were then scored for cleavage furrow regression, delayed abscission, or no abscission (as in Table 1) and were additionally scored for apoptotic cells by scoring cells that were actively blebbing, and subsequently collapsed and became nonrefractile during the period of observation.

seen; our unpublished data). After HEF1 depletion in asynchronous cells, the fluorescence-activated cell sorting (FACS) profile was generally similar to that of control cells, with a small but consistent >4N peak that might indicate failure of karyokinesis (Figure 2B, arrow). In spite of the relatively normal FACS profile, cells with depleted HEF1 had several hallmarks of defects in mitotic entry. Staining with antibody to phosphorylated Histone H3, an indicator of mitotic entry, was consistently lower in HEF1-depleted cells versus controls (0.5% positive cells with HEF1 depletion versus 3.4% positive in controls). In cells treated with HEF1-targeting siRNA, consistently only 50% as many cells were

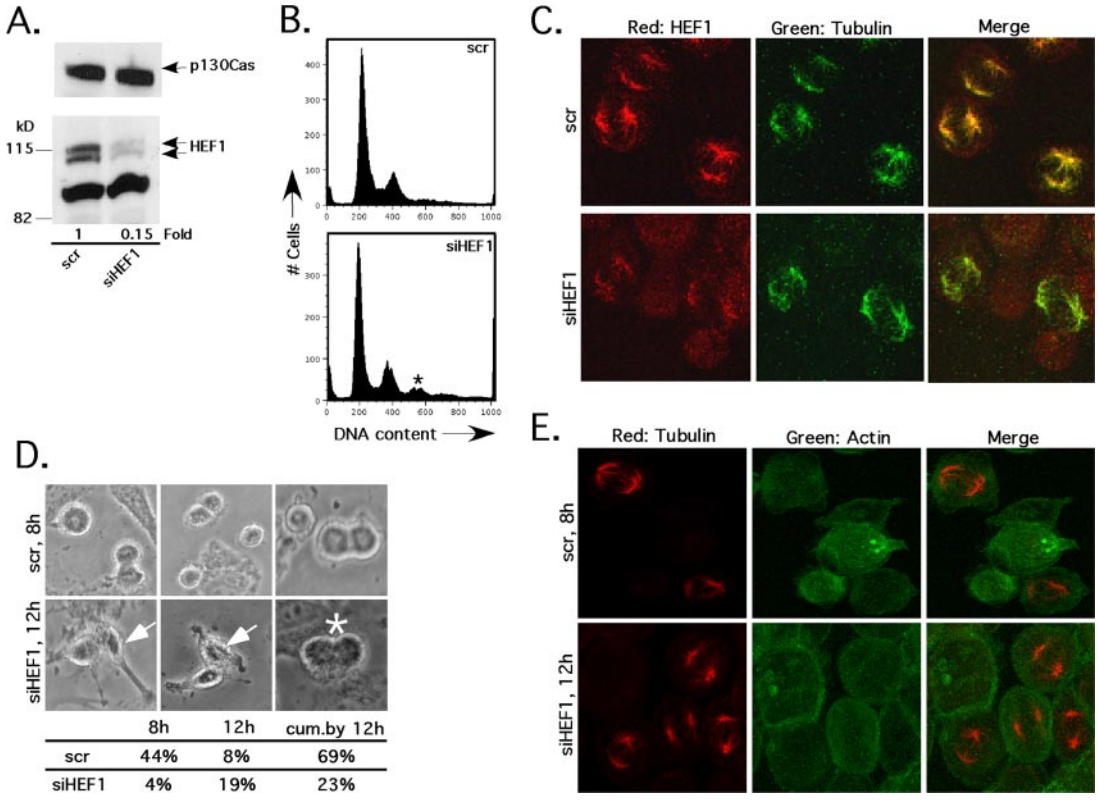

Figure 2. siRNA depletion of HEF1. (A) Depletion of HEF1 protein by siRNA treatment. Western blot analysis of HEF1 protein levels after treatment with siRNA. scr, MCF-7 cells transfected with a scrambled siRNA. siHEF1, MCF-7 cells transfected with siRNA directed against HEF1. Cell lysates were collected 48 h after transfection and immunoblotted with anti-HEF1 and anti-p130Cas antibody to show specific depletion. Quantitation of images indicates >85% depletion of HEF1 expression in the experiment shown: the typical range of depletion for data reported in this manuscript is 80–90%. (B) Flow cytometric analysis of asynchronous cells 48 h posttransfection with control scrambled (scr, left) or HEF1-targeted (siHEF1, right) siRNAs. Asterisk indicates >4N peak. (C) Immunofluorescence of MCF-7 cells synchronized with double thymidine block, treated during block with siRNA to HEF1 or control (Scr), 8 or12 h after release, as indicated. HEF1 is shown in red; α-tubulin in green. (D) Phase micrographs of synchronized thymidine-blocked MCF-7 depleted for HEF1 or control (Scr), 8–12 h postrelease (as indicated). Arrows indicate cells with clear metaphase plates but maintaining attachment. Asterisk demonstrates HEF1-depleted cell with separated DNA, lacking cleavage furrow. Quantitation represents the percentage of cells observed rounded for mitosis at each time point as well as the total percentage observed as mitotic within 12 h after release from block. (E) Immunofluorescence of MCF-7 cells synchronized with double thymidine block, treated during block with siRNA to HEF1 or control (Scr). α-Tubulin is shown in red; actin in green. Maximal rounding of Scr-depleted cells is shown at 8 h, for HEF1-depleted at 12 h.

Table 3. M-phase defects accompanying HEF1 depletion and manipulation of ECT2 and RhoA

Cell line	Unable to form cleavage furrow (%)	Cleavage furrow regression (%)	No abscission (%)
Effect of siHEF1			
MCF-7(scr)	0	3	0
MCF-7(siHEF1)	19	22	0.8
MCF-7(siECT2)	17	20	0
Effect of siECT2			
HEF1.M1(+T)	0	1	0
HEF1.M1(+T) + siECT2	15	18	2.8
HEF1.M1(−T)	0	14	22
HEF1.M1(−T) + siECT2	0	3	2
Effect of RhoA-L63			
MCF-7(vector)	1	0	0
MCF-7(HEF1)	0	5	37
MCF-7(RhoA-L63)	0	7.5	20

Experiments performed as in Tables 1 and 2; see text for details.

obtained in mitotic shake-offs versus cells with scrambled siRNA treatment, suggesting initial difficulty with rounding or detachment. Videomicroscopic analysis of HEF1-depleted cells (Table 3) confirmed deficiencies in HEF1 progress through mitosis but at a different stage than seen with HEF1 overexpression. Nineteen percent of HEF1-depleted cells that rounded up did not form a detectable cleavage furrow, whereas 22% exhibited cleavage furrow regression, and appearance of binucleate cells.

We next examined the consequences of HEF1 depletion in synchronized cells. MCF-7 cells were synchronized by double thymidine block, with siRNA treatment concurrent with the second thymidine treatment, and then released and examined by time-lapse microscopy for the next 12 h for cell rounding and entry into mitosis. HEF1 was efficiently depleted in these cells (Figure 2C) with signal much reduced at the mitotic spindles in cells entering mitosis. However, HEF1-depleted synchronized cells took longer to round up than control-depleted cells, and many fewer cells rounded up even at later time points (Figure 2, D and E). At 8 h after release from nocodazole, 44% of control-depleted cells were rounded, whereas 4% HEF1-depleted cells were rounded; cumulatively over the experiment, observed rounding was 69% (control-depleted cells) versus 23% (HEF1-depleted cells). Based on scrutiny at high magnification, many of the cells had entered mitosis, based on the presence of visible bipolar mitotic spindles; however, the number of cells with detectable spindles was reduced relative to control-depleted cells, and the spindles were in many cases poorly formed. Notably, HEF1-depleted cells maintained more attachments to the tissue culture plate than control-depleted cells, and as with unsynchronized cultures, had a high proportion of cells that did not form cleavage furrows or that exhibited cleavage furrow regression. Together with the overexpression studies, these results suggested that HEF1 activity might contribute to early stages of mitotic progression but needs to be down-regulated or eliminated at late stages to allow cell separation.

Localization of HEF1 to Mitotic Structures

Before M phase, HEF1 localizes to focal adhesions and to the centrosomes (Fashena *et al*., 2002; Pugacheva and Golemis, 2005). To more exactly analyze the HEF1 control mechanisms in mitosis, the localization of endogenous (Figure 3A) HEF1 was examined from early M phase through cytokinesis, to establish point of action. After localization at the mitotic spindle in early and mid-M phase, HEF1 subsequently moves to the central spindle. As cytokinesis ap-

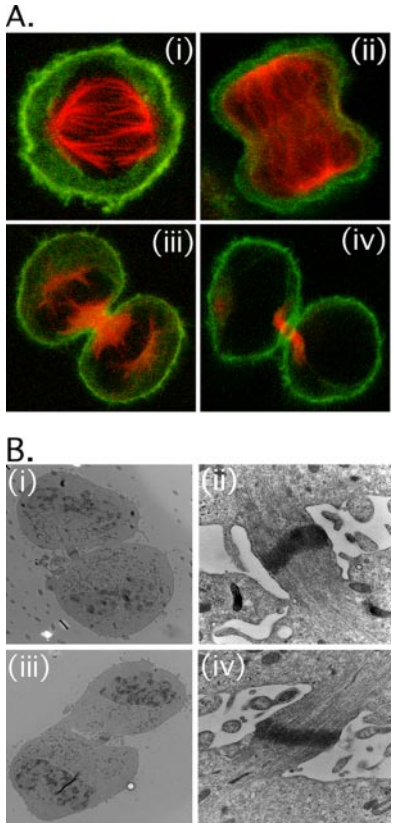

Figure 3. HEF1 localization and ultrastructure of HEF1-induced cells at abscission. (A) M-phase localization of endogenous HEF1 in MCF-7 cells (left). Cells are examined at i) metaphase, ii) anaphase, iii) telophase, and iv) at the point of abscission. Red, HEF1; green, actin. (B) Normal ultrastructure at the stage of abscission in the presence or absence of overexpressed HEF1. Electron micrograph of the postmitotic bridge at low (i and iii, left) and high (ii and iv, right) magnification in CM1 cells (i and ii, top) or HEF1.M1 cells (iii and iv, bottom) in absence of tetracycline.

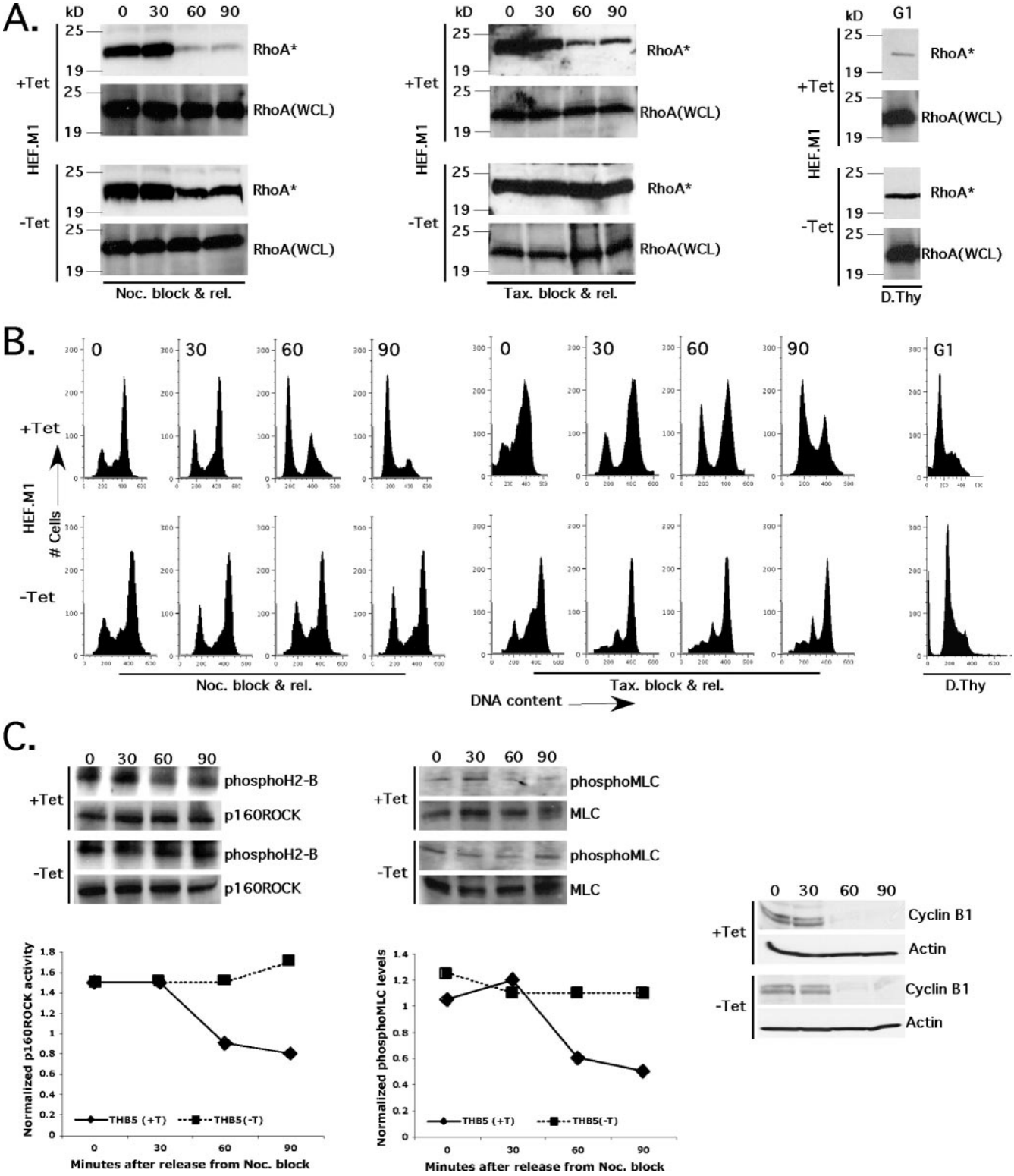

Figure 4. HEF1 controls the RhoA activation cycle. (A) Overexpression of HEF1 induces persistent activation of RhoA. RhoA activation was assessed in cells collected by mitotic shake-off after synchronization with thymidine and subsequent nocodazole or taxol treatment at indicated time points 0, 30, 60, and 90 min after release from both nocodazole (Noc., left) or taxol (Tax., middle) or maintained in double thymidine block (G_1, right). HEF1.M1 grown in the presence (+Tet) and absence (−Tet) of tetracycline are shown. RhoA* represents activated RhoA pulled down by GST-RBD, and RhoA (WCL) represents total RhoA in whole cell lysate: each is visualized by antibody to RhoA. HEF1-overexpressing cells showed persistent activation of RhoA at 60 and 90 min when released from either nocodazole (left) or taxol (middle). Similar results were obtained in three independent experiments, and a representative blot is shown. (B) Flow cytometry analysis of HEF1.M1 cells prepared as described in Fig. 4A, after release from nocodazole (left) or taxol (middle) or maintained in double thymidine block (right, G_1). (C) The activation of RhoA effectors in nocodazole-synchronized cells with uninduced (+Tet) or induced (−Tet) HEF1 was

proaches, HEF1 becomes associated with the ends of microtubules proximal to the midbody. Based on the dominant overexpression defect of failed abscission, we used electron microscopy to determine whether HEF1 overexpression in the HEF1.M1 cells (with the more severe delay phenotype) resulted in discernible disruption of the midbody and associated cytokinetic structures (Figure 3B). This analysis indicated no notable structural differences between HEF1 overexpressors and control cells at early time points after release from nocodazole (3 h), although cells trapped at abscission for extended periods manifested the characteristic ultrastructure of a postmitotic bridge, as has been seen with defects in signaling by other key cytokinetic regulatory factors (Savoian *et al*., 1999; Matuliene and Kuriyama, 2002). The lack of early structural defects in the cytokinetic apparatus suggested that HEF1 deregulation impaired signaling by such regulatory factors.

HEF1 Positively Regulates RhoA Activation

A critical control axis during mitosis and cytokinesis is timed regulation of the activation and deactivation of the RhoA GTPase (Glotzer, 2001; Maddox and Burridge, 2003), with activation of RhoA being required for cell rounding at early stages of mitosis and cleavage furrow ingression, and deactivation of RhoA being essential for abscission. The phenotypes we had observed with HEF1 depletion (reduced mitotic shake-off levels and reduced level and efficiency of cleavage furrow formation) and overexpression (abscission block) were compatible with the idea that HEF1 is a positive regulator of RhoA signaling in mitosis.

Using cells in which HEF1 is induced during thymidine block release into nocodazole block as described in *Materials and Methods*, *Cell Cycle Synchronization for HEF1 Stable Cell Lines*, the expression and activation of RhoA was analyzed for 90 min after nocodazole release (Figure 4A, left). During this time, parallel FACS analysis (Figure 4B, left) indicated the majority of cells had passed from 4N to 2N DNA content, in uninduced but not HEF1-overexpressing cells. Notably, RhoA activation was abnormally sustained throughout this period in HEF1-induced cells but not in HEF1-uninduced cells (Figure 4A, left). Compatible with the continued activation of RhoA, two different RhoA-activated effectors also showed sustained activity in HEF1-induced cells. p160ROCK immunoprecipitated from HEF1-induced cells was more active in phosphorylating Histone H2B at 60 and 90 min after release from nocodazole (Figure 4C). Similarly, more phosphorylated MLC was observed at these later time points in HEF1-induced cells (Figure 4C). Some studies have noted that use of nocodazole itself induces RhoA activation (Maddox and Burridge, 2003). We believe this is unlikely to explain the HEF1-dependent persistence of RhoA activation, because comparable starting levels of activation of RhoA, p160ROCK, and MLC are seen under HEF1-induced and uninduced conditions (compare Figure 4, A and C, left, time point 0). Nevertheless, we wanted to evaluate cells inhibited by different means. Although the proteasomal inhibitor MG132 has been reported to efficiently synchronize some cells at metaphase (Genschik *et al*., 1998), it did not efficiently induce arrest in MCF-7 cells (our unpublished data). Taxol-induced cell cycle arrest was effective (Figure 4B, middle), and indicated a similar HEF1-dependent delay in passage from 4N to 2N, and a similar persistence in levels of activated RhoA in cells at 60 and 90 min after release from cell cycle arrest (Figure 4A, middle). We note that recovery from taxol is known to be slower than recovery from nocodazole arrest; this is likely to explain the slight delay in progression from 4N to 2N in taxol-treated cells (compare Figure 4B, left and middle).

Together, these results indicated that either HEF1 expression delayed progression through stages of mitosis before cytokinesis, which is unlikely because our videomicroscopic analysis did not detect delays in progression through stages before abscission and because cyclin B1 levels declined at comparable time points in HEF1-induced and -uninduced cells (Figure 4C, right), or HEF1 overexpression caused persistent RhoA activation at a cell cycle phase at which it is normally down-regulated. Finally, for comparison, we also determined levels of RhoA activation in nonmitotic cells arrested with double thymidine block in the presence and absence of HEF1 induction (Figure 4A, right, and B, right). We note, increased levels of HEF1 also promoted some increase in the levels of RhoA in G_1/S-arrested cells, although this was not as large as observed in mitotic cells.

HEF1 Promotes the Persistence of ECT2 Activation in Late Mitosis

We wanted to specifically understand the mechanistic basis of HEF1 induction of RhoA activation in mitosis. The activation cycle of RhoA is specified by interactions with the protein ECT2 (Kimura *et al*., 2000) (a DBL-family GTP exchange factor [GEF] and an orthologue of the critical *Drosophila* cytokinetic regulator Pebble, O'Keefe *et al*., 2001), which promotes RhoA activation, and by other proteins, notably RhoA-GTPase-activating protein (GAPS), involved in RhoA inactivation later in mitosis. The ECT2 GDP-GEF is abundant in G_2/M and promotes the activation of RhoA in mitosis, whereas hyperactivation of ECT2 has been reported to cause cytokinesis defects (Tatsumoto *et al*., 1999; Kimura *et al*., 2000; Saito *et al*., 2003). To investigate ECT2 as intermediary between HEF1 and RhoA, we used two different commercial antibodies to ECT2 (Santa Cruz Biotechnology). HEF1 overexpression caused persistence of ECT2 levels in late mitosis (Tatsumoto *et al*., 1999), compatible with promotion of prolonged RhoA activation (Figure 5A; our unpublished data). Furthermore, ECT2 showed a strongly enhanced localization to the midbody in HEF1-overexpressing cells at the point of cytokinesis (Figure 5B), adjacent to the concentrated HEF1 at the proximal microtubule bundles (Figure 2A). We next examined whether HEF1 and ECT2 might directly interact. We found that in cells co-overexpressing epitope-tagged HEF1 and ECT2, antibody to tagged-ECT2 efficiently coimmunoprecipitated HEF1 (Figure 5C, i), whereas antibody to tagged-HEF1 also efficiently immunoprecipitated epitope tagged-ECT2 (Figure 5C, ii). Furthermore, antibody to ECT2 coimmunoprecipitated endogenous ECT2 with endogenous HEF1 from both asynchronous and mitotic cell lysates (Figure 5D). Interestingly, the hyperphosphorylated p115 form of HEF1 precipitated more efficiently with ECT2 than did the hypophosphorylated p105 form. We (Law *et al*., 1998; Pugacheva and Golemis, 2005) and others have noted that p115 HEF1 is enriched

Figure 4 (cont). examined after release from nocodazole block. Left, p160ROCK was immunoprecipitated, total levels were determined by Western (p160ROCK), and used for kinase assay with a Histone H2B substrate, followed by visualization with a phospho-H2B-specific antibody, to determine activity. Middle, whole cell lysates were probed with antibody to phosphorylated (phospho-MLC) or total MLC. Below each set of Western blots, quantitation of relative levels of phosphorylated H2B and MLC in Tet+ and Tet− cells. Right, expression of Cyclin B1 in cells at comparable time points after release from nocodazole. Blots were stripped and reprobed with actin to confirm equal load.

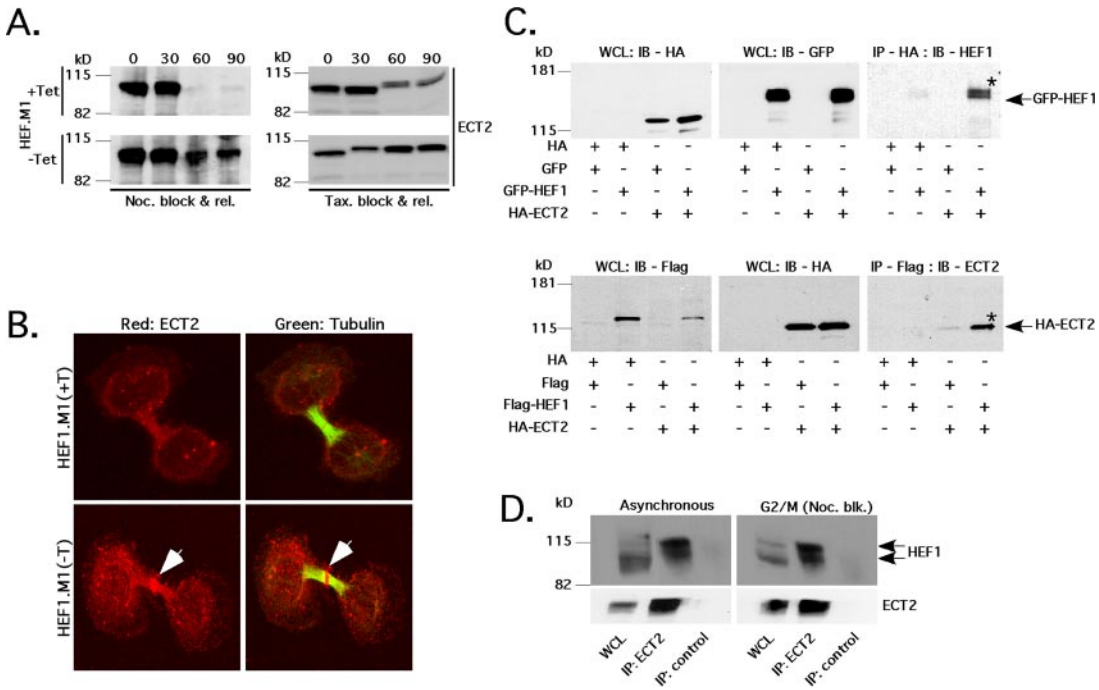

Figure 5. HEF1 positively regulates RhoA activation and associates with ECT2 during M phase. (A) Overexpression of HEF1 causes persistence of ECT2 in the late stages of M phase. Cell lysates from HEF1.M1 in the presence (+Tet) and absence (−Tet) of tetracycline were prepared as described in Figure 4A, and immunoblotted with α-ECT2 antibody. Overexpression of HEF1 leads to persistence of ECT2 in mitotic cells released from either nocodazole (left) or taxol (right). (B) HEF1 overexpression leads to persistence of ECT2 (see arrow) at the midbody during anaphase. HEF1.M1 cell line, in the presence (top) and absence (bottom) of tetracycline. Red, ECT2; green, α-tubulin. (C) Epitope-tagged HEF1 and ECT2 reciprocally coimmunoprecipitate. Cell lysates from cells cotransfected with epitope-tagged HEF1 and ECT2, or negative vector controls, were either directly analyzed by Western blot as WCL, or subjected to IP using the antibodies as indicated, followed by immunoblotting (IB) with the specified antibodies. For i and ii, left two panels represent WCL directly probed by Western; extreme right panel shows immunoprecipitates probed with antibody against the coimmunoprecipitated protein; i, α-HA antibody was used to immunoprecipitate HA-ECT2 containing complexes, and immunoprecipitates were probed with α-HEF1; WCL were probed with α-HA and α-GFP. Lane 1, pCDNA6HA and pEGFP-HEF1; lane 2, pCDNA6HA-pEGFP-HEF1; lane 3, pCDNA6HA-ECT2 and pEGFP; and lane 4, pCDNA6HA-ECT2 and pEGFP-HEF1. ii, α-Flag antibody was used to immunoprecipitate Flag-HEF1 containing complexes, and immunoprecipitates were probed with α-ECT2; WCL were probed with α-Flag and α-HA. Lane 1, pCDNA6HA and pCatchFlag; lane 2, pCDNA6HA-pCatchFlag-HEF1; lane 3, pCDNA6HA-ECT2 and pCatchFlag; and lane 4, pCDNA6HA-ECT2 and pCatchFlag-HEF1. Asterisk (*) indicates immunoprecipitated protein. (D) Endogenous ECT2 preferentially immunoprecipitates with hyperphosphorylated HEF1. Whole cell lysates from asynchronous or nocodazole arrested MCF-7 cells were directly loaded to an SDS-PAGE gel (WCL), or 1 mg of lysate was used for immunoprecipitation with antibody to ECT2 or a negative control sera from nonimmunized rabbits (control). Blots were visualized with antibody to HEF1 or to ECT2.

in G_2/M cells, suggesting HEF1 may be most able to interact with ECT2 in these phases of cell cycle.

We next examined whether depletion of HEF1 negatively regulated activation of RhoA and ECT2 levels (Figure 6A). Treatment with HEF1-targeting siRNA in cells synchronized with nocodazole to enrich the mitotic cell population resulted in significant reductions in RhoA activation (Figure 6A, top, siHEF1 lane). Cells were comparably synchronized at times of assay (Figure 6B). HEF1 depletion also reduced levels of ECT2 in mitotic cells (Figure 6C), although the degree of depletion was not as great as for activated RhoA. Because HEF1 also reduced RhoA activation in nonmitotic cells, we next examined the consequences of HEF1 and ECT2 depletion in MCF-7 cells that had been synchronized with double thymidine block in G_1 and then released for 0, 4, 8, or 12 h (Figure 6D). At each of these time points, levels of activated RhoA were lower in HEF1-depleted cells than in cells treated with control siRNAs. Levels of RhoA were also lower in ECT2-depleted cells, but the degree of reduction was not as great as with HEF1 depletion (Figure 6D). We also observed that ECT2 signal was reduced in premitotic cells synchronized with double thymidine block and release depleted for HEF1 (Figure 6E), or in asynchronous cell populations not treated with any drug (Figure 6F). The simplest explanation for our results in sum is that association of HEF1 with ECT2 stabilizes ECT2 and that overexpression of HEF1 allows activated mitotic ECT2 to compete more efficiently with RhoA-GAPs to maintain RhoA activation at the midbody before cell separation, causing a cytokinetic defect.

Inhibition of RhoA Activation Reverses the Cytokinetic Block Induced by HEF1 Overexpression

To establish whether HEF1 regulation of RhoA is critical for HEF1-dependent mitotic phenotypes, we tested whether inhibitors of RhoA (the enzyme C3 transferase) or the RhoA effector p160ROCK (Y-27632) were able to promote abscission in cells with induced HEF1 (Figure 7, A and B). At 3 h after release from taxol (Figure 7A) or nocodazole (our unpublished data), almost all uninduced HEF1.M1 cells had progressed through cytokinesis into G_1, whereas a significant number of induced HEF1.M1 cells remained joined by a postmitotic bridge. However, addition of either C3 transferase or Y-27632 to the culture medium caused the rapid flattening of these joined cells, with effects noticeable within

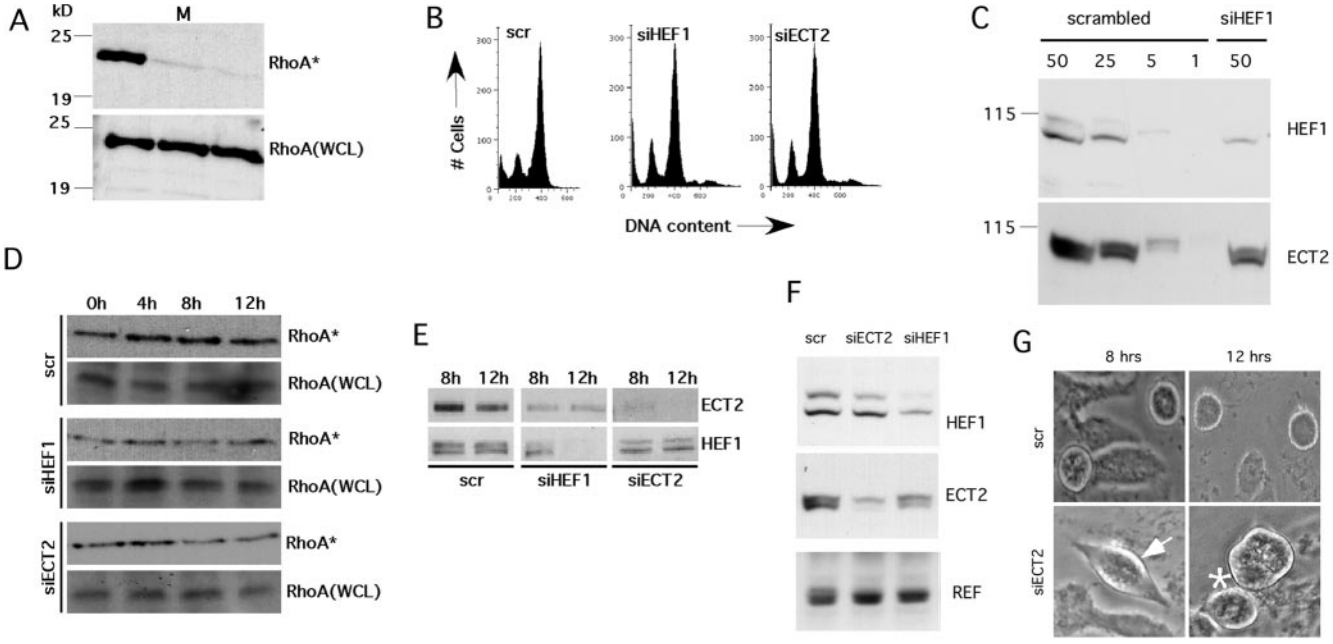

Figure 6. Depletion of HEF1 inhibits RhoA activation and ECT2 expression. (A) HEF1 depletion causes hypoactivation of RhoA in mitotic cells. Cell lysates were prepared from nocodazole-blocked cells (M) that have been treated with a scrambled siRNA (scr) or with siRNA targeted to HEF1 (siHEF1) or ECT2 (siECT2). Cell lysates were probed for presence of activated RhoA or total RhoA (assessed as in Figure 4A). (B) FACS profiles of nocodazole-arrested cells treated with scrambled oligo (left), siHEF1 (middle), and siECT2 (right) and indicate equivalent cell synchronization of all the treated cells. (C) HEF1 depletion reduces steady-state levels of ECT2 in mitotic cells. Cells were prepared as in A after treatment with scrambled siRNA, or siRNA to HEF1, and lysates were probed with antibody to HEF1 (top) or ECT2 (bottom). Fifty (50), 52, 5, and 1 denote micrograms of lysate loaded per lane, to allow a visual measure of degree of depletion. (D) HEF1 or ECT2 depletion reduces activation of RhoA in interphase cells. Synchronized thymidine-blocked MCF7 depleted for HEF1, ECT2 or control (Scr) were released from block, and RhoA activation assessed for 0–12 h after release. Degree of HEF1 and ECT2 depletion was confirmed by parallel Western blots. (E) Reduction of HEF1 or ECT2 levels in double thymidine blocked cells 8 or 12 h after release, in experiment described in D. (F) Depletion of HEF1 causes a reduction in ECT2 levels in untreated asynchronous cells. Lysates of cells treated with siRNA as described in A were resolved by SDS-PAGE and probed with antibodies indicated to HEF1 or ECT2: a nonspecifically hybridizing band provides a loading control (REF). (G) Phase micrographs of synchronized thymidine-blocked MCF-7 depleted for ECT2 or control (Scr), 8–12 h postrelease, as indicated. Arrow and asterisk indicate a mitotic cell that fails in cleavage furrow ingression.

10 min, and dramatic by 30 min. These morphological changes were paralleled by FACS analysis, which indicated that cells had moved from 4N to 2N DNA content (Figure 7B). These results buttressed the significance of RhoA activation as a mediator of HEF1 function in mitosis and additionally allowed us to conclude that the effect induced by HEF1 was a reversible, rather than terminal, signaling defect.

Direct Manipulation of RhoA and ECT2 Produces Mitotic Defects Compatible with a Model in Which They Are Positively Regulated by HEF1

As final tests of the importance of ECT2 and RhoA function for HEF1 activity in mitosis, we used videomicroscopy to analyze the consequences of manipulating ECT2 or RhoA, in the presence or absence of HEF1 manipulation (Figure 6G and Table 3; our unpublished data). We found that depletion of ECT2 by siRNA, whether in parental MCF-7 cells or in uninduced HEF1.M1 cells, induced phenotypes comparable with depletion of HEF1. Only 20% of ECT2-depleted cells have rounded for mitosis by 8 h after thymidine block, and a cumulative total of 29% by 12 h (compare with Figure 2D). ECT2 cells that rounded commonly failed to form cleavage furrow, or displayed cleavage furrow regression. Similar results were obtained in asynchronously growing depleted cells, and cells that were depleted after synchronization in double thymidine block. Depletion of ECT2 in induced HEF1.M1 cells markedly decreased the severity of the HEF1-dependent abscission block; in fact, cells induced to express HEF1, but depleted for ECT2, were similar to control cells. In a reciprocal experiment, plasmids expressing constitutively active RhoA (RhoA-L63) or HEF1 were cotransfected with a plasmid expressing GFP in parallel into MCF-7 cells, and the phenotypes of GFP-positive cells were scored (Table 3). As with HEF1, RhoA-L63 induced a phenotype in which cells were blocked at the point of abscission. In sum, these results confirmed the interdependence of HEF1, ECT2, and RhoA function in mitosis.

DISCUSSION

As a current model for HEF1 action in M phase, we propose that in normal cells, HEF1 activity promotes the early stages of mitotic rounding and cleavage furrow ingression. HEF1 promotes these processes by contributing to RhoA activation, thereby increasing cortical rigidity and cortical retraction (Maddox and Burridge, 2003). Defects in ECT2 have previously been associated with defective contractile ring function and failed cytokinesis (Prokopenko *et al.*, 1999, 2000; Tatsumoto *et al.*, 1999; Kimura *et al.*, 2000). Our data are compatible with the idea that HEF1 normally associates with ECT2 and enhances activation of RhoA in early M phase, but HEF1 activation of ECT2 is diminished during cytokinesis,

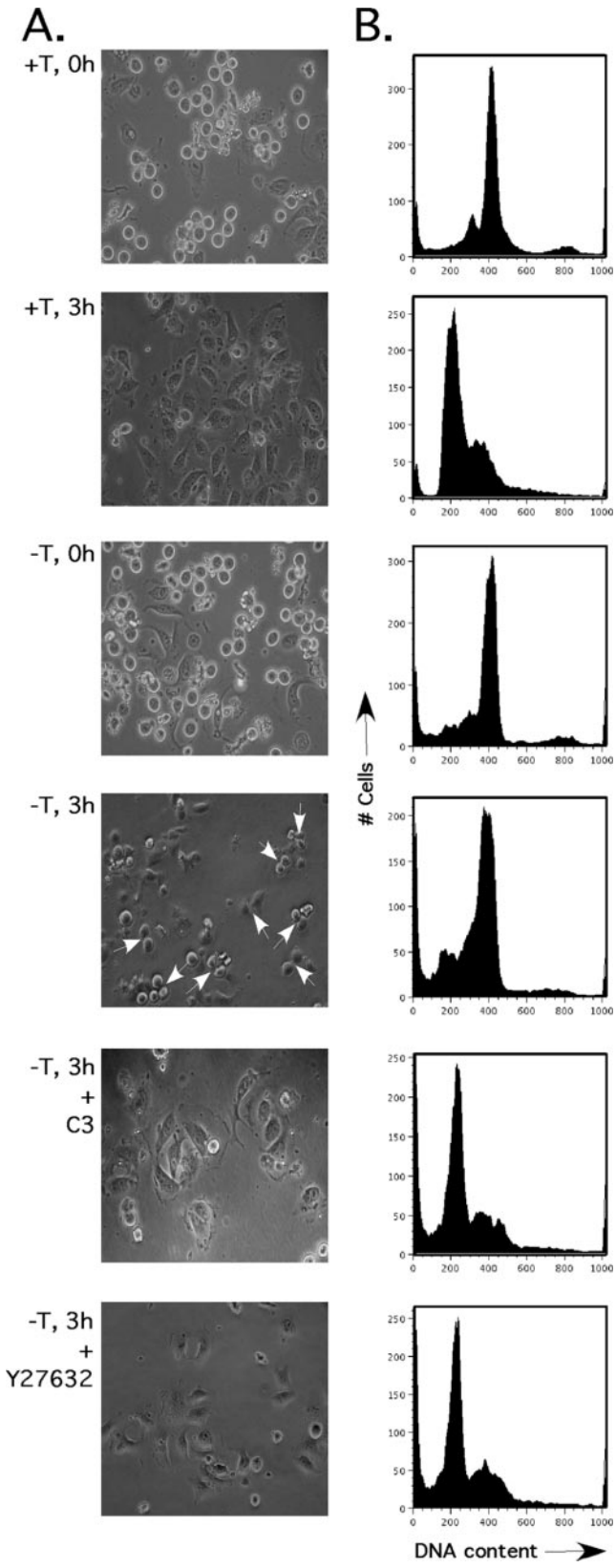

causing negative regulators of RhoA to become dominant in their interactions with RhoA, allowing abscission. In this model, overxpression of HEF1 causes a block at abscission by maintaining levels of RhoA activation: cells proceeding through this block tend to be aneuploid and have supernumerary centrosomes, compatible with the phenotypes described by us in (Pugacheva and Golemis, 2005). Conversely, depletion of HEF1 reduces the frequency of cell rounding for mitosis, and inhibits cleavage furrow formation, at least in part by depressing RhoA activation, although the disorganized spindles found in many HEF1-depleted mitotic cells also suggest that activation of a spindle checkpoint may also contribute to the earlier mitotic failure of these cells.

It is becoming increasingly clear that the regulated activation and inactivation of RhoA is of central importance to the physical rearrangements that occur in mitosis (reviewed in Glotzer, 2001), with data supporting this interpretation arising in model systems ranging from yeast, worms, and flies to vertebrates. At present, the exact mechanism by which RhoA acts is not completely clear, with different groups presenting conflicting results. As one example, Burridge and coworkers have reported that RhoA activation is highest in early mitosis, gradually reducing in later stages (Maddox and Burridge, 2003), whereas Narumiya and colleagues have reported a very different pattern, with RhoA levels gradually rising through mitosis to reach their highest levels in telophase (Kimura *et al*., 2000). Recently, one study has identified cell type-specific differences in RhoA activation, and requirement for RhoA in cytokinesis (Yoshizaki *et al*., 2004), which may explain some of the discrepancies. The data presented here are in general agreement with those generated by the Burridge group, indicating RhoA is normally most active in early mitosis, but it becomes less active as cells approach abscission. However, the presence of such differences in the context of the unquestionable importance of RhoA signaling controls makes further investigation of the relevant mechanisms critical.

Our data, documenting 1) similar phenotypes of HEF1 and ECT2 depletion; 2) the ability of ECT2 depletion to reduce cytokinetic block in cells induced to overexpress HEF1; 3) the overlapping localization of HEF1 and activated ECT2 at abscission, 4) the increase in levels of ECT2 at the midbody in the context of HEF1 overexpression; 5) the efficient and reciprocal coimmunoprecipitation of hyperphosphorylated HEF1 and ECT2; and 6) the reduction in steady-state levels of ECT dependent on depletion of HEF1 (typically, 2- to 3-fold) together strongly imply that ECT2 mediates some of HEF1 regulation of RhoA in mitosis. There is a clear evolutionarily conserved function of ECT2/Pebble/LET-21 in regulation of RhoA and cleavage furrow formation (Dechant and Glotzer, 2003) and cytokinesis (O'Keefe *et al*., 2001), first documented in lower eukaryotes. Subsequent studies of ECT2 in vertebrates have documented the importance of this protein in similar processes in higher eukaryotes (Saito *et al*., 2003; Tatsumoto *et al*., 2003), supporting earlier work from the same group (Tatsumoto *et al*., 1999). However, reduction of ECT2 levels based on HEF1 depletion may not completely explain the reduced activity

Figure 7. Inhibition of RhoA or p160ROCK kinase activity rescues the defect in persistent rounding and abscission caused by HEF1 overexpression. (A) HEF1.M1 cells in the presence (+T) and absence (−T) of tetracycline were arrested with nocodazole (0 h) and released from the taxol block for 3 h (3 h). Numerous cells trapped before abscission are seen in (−T; 3 h) cells, indicated by arrows. C3 transferase protein (C3) or Y-27632 was added to the −T, 3 h HEF1.M1 cells, and observed after 30 (C3) or 10 (Y-27632) min. Addition of either of the inhibitors allowed the cells to undergo abscission and spread. (B) FACS profile of the cells shown in A. Treatment with either C3 transferase or Y-27632 induces movement of cells from 4N stage to 2N.

of RhoA in cells treated with siRNA to HEF1, because less HEF1-dependent reduction of ECT2 than active RhoA is observed (although caution is needed when making extrapolations from changes in total protein levels versus activated protein levels).

Beyond ECT2, RhoA activation is controlled by numerous activator GEFs and inhibitor GAPs (Van Aelst and D'Souza-Schorey, 1997; Maddox and Oegema, 2003). Some of these are active in mitosis, and others are not. Data presented here indicate that HEF1 also partly regulates RhoA activation in cells that are not in mitosis (Figures 4 and 6D), a time at which ECT2 has been described as relatively inactive (Kim *et al*., 2005). An increasing number of studies have indicated cross-talk between the integrin-dependent attachment machinery and RhoA (see below), and it is likely that the HEF1 and the other Cas proteins (p130Cas and Efs) as central downstream components of the integrin cascade, will play a role in this process. Of other well-studied RhoA-regulators, previous work has suggested that p190GAP does not play an important role in RhoA mitotic functions (Maddox and Burridge, 2003). The CYK-4/MgcRACGAP protein (Jantsch-Plunger *et al*., 2000; Minoshima *et al*., 2003) has a very significant function in the down-regulation of RhoA activity in late M phase. Our preliminary data indicate that the gross levels of MgcRACGAP do not change in response to manipulation of HEF1 levels (our unpublished data), but we have not yet investigated possible changes in the activity of this protein.

Other work from our group has recently shown that HEF1 binds and activates the Aurora-A kinase at mitotic entry (Pugacheva and Golemis, 2005). Overexpression or constitutive activation of Aurora-A, results after one or two division cycles in supernumerary centrosomes and multipolar mitotic spindles, dependent on an initial failure of cytokinesis: this is thought to be an important predetermining factor for genomic instability in many cancers (Marumoto *et al*., 2005). Although the mechanism by which Aurora-A amplification promotes cytokinetic failure remains to be determined, interestingly, Aurora-A and the RhoA effector p160ROCK have been shown to form a complex in mitotic cells, and siRNA depletion of p160ROCK blocked some Aurora-A-dependent defects (Du and Hannon, 2004). Hence, the association of HEF1 with Aurora-A provides a separate means by which Aurora-A might influence RhoA. To date, our experiments indicate that although HEF1 interacts with ECT2, and interacts with Aurora-A, ECT2 and Aurora-A do not stably associate with each other; rather, it seems likely that HEF1 associates with Aurora-A in G_2 and at the initiation of M, then this complex dissociates, and HEF1 becomes available to associate with ECT2 (our unpublished data). The regulation of ECT2 in mitosis is increasingly appreciated to be complex, involving mitotic-specific phosphorylation and the exchange of intra- and intermolecular protein interactions (Tatsumoto *et al*., 1999, 2003; Saito *et al*., 2003, 2004; Liu *et al*., 2004; Solski *et al*., 2004; Kim *et al*., 2005). Hence, it is also possible that HEF1 modulates some of these ECT2-related control pathways, for example, by altering the phosphorylation and thereby protein interactions and activation of ECT2. At present, it seems likely that both ECT2 and Aurora-A may contribute to HEF1 overexpression-dependent mitotic defects, and it would be of interest to further examine ECT2 as a potential mediator of the cytokinetic failure induced by Aurora-A.

HEF1 and its close family members p130Cas and Efs/Sin are also important mediators of signaling related to attachment, motility, and apoptosis (O'Neill *et al*., 2000). We and others have also previously determined that overexpression of HEF1 impacts cell spreading, causing initial enhancement of spreading, and subsequent retraction (O'Neill and Golemis, 2001; van Seventer *et al*., 2001; Fashena *et al*., 2002). Defective cellular attachment can independently result in cytokinetic failure (Orly and Sato, 1979; Ben-Ze'ev and Raz, 1981), and it is well established in some models that force generation arising from spreading at the end of telophase assists in cytokinesis (Burton and Taylor, 1997; Gerald *et al*., 1998; Nagasaki *et al*., 2002). However, we have determined that plating HEF1-induced cells on fibronectin or laminin to enhance cell spreading had no appreciable effect on the frequency of defective cytokinesis or number of rounded cells with persistent post-mitotic bridges (our unpublished data). This result indicates the HEF1-induced defect is dominant to extrinsic signals promoting cell attachment. At present, it remains possible that inadequate traction may contribute to the cytokinetic phenotypes observed.

Enlarging on this last point, and as stated above, a growing set of proteins associated with focal adhesions, including the integrins, FAK, and others have been shown to be engaged in a reciprocal regulatory dialog with RhoA in control of cell attachment and cell motility during interphase (Flinn and Ridley, 1996; Arthur *et al*., 2000; Ren *et al*., 2000; Schwartz and Shattil, 2000; Sinnett-Smith *et al*., 2001; Arthur *et al*., 2002; Danen *et al*., 2002). FAK (−/−) null cells are nonmotile and excessively rounded; however, inhibition of p160ROCK in FAK(−/−) cells reverses rounding, implying FAK functions are dependent on RhoA (Chen *et al*., 2002). The HEF1 protein is a physical partner of FAK (Law *et al*., 1996), making it well positioned to take part in such regulatory networks; furthermore, recent studies suggest HEF1 is itself a target of RhoA regulation in cell attachment (Bargon *et al*., 2005). The focal adhesion protein zyxin is also of considerable interest in this context. Like HEF1, zyxin transits from focal adhesion to the mitotic spindle in mitosis (Hirota *et al*., 2000). Zyxin and HEF1 have been shown to physically interact (Yi *et al*., 2002). Finally, in a recent study of the consequences of zyxin depletion, the most noticeable phenotype was the loss of stress fibers; stress fibers are under the control of RhoA (Ridley and Hall, 1992). The demonstration in this report that HEF1 regulates RhoA signaling in mitosis suggests that cell economically reutilizes the interphase actin regulatory machinery during mitosis to assist in control of the dramatic changes in cytoskeletal organization associated with cell separation. Coupled with recent reports that integrins themselves regulate Cdc2/cyclin B to promote cell motility (Manes *et al*., 2003), these results support the idea of extensive cross-talk between cell attachment and cell division controls.

ACKNOWLEDGMENTS

We are grateful to Dr. Geraldine O'Neill for communicating results before publication. Drs. Elizabeth Henske, Geraldine O'Neill, and Jonathan Chernoff provided useful comments on the manuscript. This work was supported by National Institutes of Health Grant CA63366 and Tobacco Settlement funding from the State of Pennsylvania (to E.A.G.), by funding from the Susan B. Komen Foundation, and by a National Institutes of Health Core Grant CA-06927 to Fox Chase Cancer Center. Disha Dadke was supported by a Plain and Fancy Fellowship. Elena Pugacheva was supported by a Department of Defense Training grant in Breast Cancer.

REFERENCES

Alexandropoulos, K., and Baltimore, D. (1996). Coordinate activation of c-Src by SH3- and SH2-binding sites on a novel, p130Cas-related protein, Sin. Genes Dev. *10*, 1341–1355.

Arthur, J. S., Elce, J. S., Hegadorn, C., Williams, K., and Greer, P. A. (2000). Disruption of the murine calpain small subunit gene, Capn 4, calpain is

essential for embryonic development but not for cell growth and division. Mol. Cell. Biol. *20*, 4474–4481.

Arthur, W. T., and Burridge, K. (2001). RhoA inactivation by p190RhoGAP regulates cell spreading and migration by promoting membrane protrusion and polarity. Mol. Biol. Cell *12*, 2711–2720.

Arthur, W. T., Noren, N. K., and Burridge, K. (2002). Regulation of Rho family GTPases by cell-cell and cell-matrix adhesion. Biol. Res. *35*, 239–246.

Bargon, S. D., Gunning, P. W., and O'Neill, G. M. (2005). The Cas family docking protein, HEF1, promotes the formation of neurite-like membrane extensions. Biochim. Biophys. Acta *1746*, 143–154.

Ben-Ze'ev, A., and Raz, A. (1981). Multinucleation and inhibition of cytokinesis in suspended cells: reversal upon reattachment to a substrate. Cell *26*, 107–115.

Boudreau, N., and Bissell, M. J. (1998). Extracellular matrix signaling: integration of form and function in normal and malignant cells. Curr. Opin. Cell Biol. *10*, 640–646.

Bouton, A. H., Riggins, R. B., and Bruce-Staskal, P. J. (2001). Functions of the adapter protein Cas: signal convergence and the determination of cellular responses. Oncogene *20*, 6448–6458.

Burton, K., and Taylor, D. L. (1997). Traction forces of cytokinesis measured with optically modified elastic substrata. Nature *385*, 450–454.

Chen, B. H., Tzen, J. T., Bresnick, A. R., and Chen, H. C. (2002). Roles of Rho-associated kinase and myosin light chain kinase in morphological and migratory defects of focal adhesion kinase-null cells. J. Biol. Chem. *277*, 33857–33863.

Cos, S., Fernandez, F., and Sanchez-Barcelo, E. J. (1996). Melatonin inhibits DNA synthesis in MCF-7 human breast cancer cells in vitro. Life Sci. *58*, 2447–2453.

Danen, E. H., Sonneveld, P., Brakebusch, C., Fassler, R., and Sonnenberg, A. (2002). The fibronectin-binding integrins alpha5beta1 and alphavbeta3 differentially modulate RhoA-GTP loading, organization of cell matrix adhesions, and fibronectin fibrillogenesis. J. Cell Biol. *159*, 1071–1086.

Dechant, R., and Glotzer, M. (2003). Centrosome separation and central spindle assembly act in redundant pathways that regulate microtubule density and trigger cleavage furrow formation. Dev. Cell *4*, 333–344.

Du, J., and Hannon, G. J. (2004). Suppression of p160ROCK bypasses cell cycle arrest after Aurora-A/STK15 depletion. Proc. Natl. Acad. Sci. USA *101*, 8975–8980.

Fashena, S. J., Einarson, M. B., O'Neill, G. M., Patriotis, C. P., and Golemis, E. A. (2002). Dissection of HEF1-dependent functions in motility and transcriptional regulation. J. Cell Sci. *115*, 99–111.

Flinn, H. M., and Ridley, A. J. (1996). Rho stimulates tyrosine phosphorylation of focal adhesion kinase, p130 and paxillin. J. Cell Sci. *109*, 1133–1141.

Fresu, M., Bianchi, M., Parsons, J. T., and Villa-Moruzzi, E. (2001). Cell-cycle-dependent association of protein phosphatase 1 and focal adhesion kinase. Biochem. J. *358*, 407–414.

Frisch, S. M., and Francis, H. (1994). Disruption of epithelial cell-matrix interactions induces apoptosis. J. Cell Biol. *124*, 619–626.

Genschik, P., Criqui, M. C., Parmentier, Y., Derevier, A., and Fleck, J. (1998). Cell cycle-dependent proteolysis in plants. Identification Of the destruction box pathway and metaphase arrest produced by the proteasome inhibitor mg132. Plant Cell *10*, 2063–2076.

Gerald, N., Dai, J., Ting-Beall, H. P., and De Lozanne, A. (1998). A role for Dictyostelium racE in cortical tension and cleavage furrow progression. J. Cell Biol. *141*, 483–492.

Glotzer, M. (2001). Animal cell cytokinesis. Annu. Rev. Cell Dev. Biol. *17*, 351–386.

Hirota, T., Morisaki, T., Nishiyama, Y., Marumoto, T., Tada, K., Hara, T., Masuko, N., Inagaki, M., Hatakeyama, K., and Saya, H. (2000). Zyxin, a regulator of actin filament assembly, targets the mitotic apparatus by interacting with h-warts/LATS1 tumor suppressor. J. Cell Biol. *149*, 1073–1086.

Inoue, H., Tavoloni, N., and Hanafusa, H. (1995). Suppression of v-Src transformation in primary rat embryo fibroblasts. Oncogene *11*, 231–238.

Ishino, M., Ohba, T., Sasaki, H., and Sasaki, T. (1995). Molecular cloning of a cDNA encoding a phosphoprotein, Efs, which contains a Src homology 3 domain and associates with Fyn. Oncogene *11*, 2331–2338.

Jantsch-Plunger, V., Gonczy, P., Romano, A., Schnabel, H., Hamill, D., Schnabel, R., Hyman, A. A., and Glotzer, M. (2000). CYK-4, A Rho family GTPase activating protein (GAP) required for central spindle formation and cytokinesis. J. Cell Biol. *149*, 1391–1404.

Kim, J. E., Billadeau, D. D., and Chen, J. (2005). The tandem BRCT domains of Ect2 are required for both negative and positive regulation of Ect2 in cytokinesis. J. Biol. Chem. *280*, 5733–5739.

Kimura, K., Tsuji, T., Takada, Y., Miki, T., and Narumiya, S. (2000). Accumulation of GTP-bound RhoA during cytokinesis and a critical role of ECT2 in this accumulation. J. Biol. Chem. *275*, 17233–17236.

Lauffenburger, D. A., and Horwitz, A. F. (1996). Cell migration: a physically integrated molecular process. Cell *84*, 359–369.

Law, S. F., Estojak, J., Wang, B., Mysliwiec, T., Kruh, G. D., and Golemis, E. A. (1996). Human Enhancer of Filamentation 1 (HEF1), a novel p130Cas-like docking protein, associates with FAK, and induces pseudohyphal growth in yeast. Mol. Cell Biol. *16*, 3327–3337.

Law, S. F., O'Neill, G. M., Fashena, S. J., Einarson, M. B., and Golemis, E. A. (2000). The docking protein HEF1 is an apoptotic mediator at focal adhesion sites. Mol. Cell Biol. *20*, 5184–5195.

Law, S. F., Zhang, Y.-Z., Klein-Szanto, A., and Golemis, E. A. (1998). Cell-cycle regulated processing of HEF1 to multiple protein forms differentially targeted to multiple compartments. Mol. Cell. Biol. *18*, 3540–3551.

Liu, X. F., Ishida, H., Raziuddin, R., and Miki, T. (2004). Nucleotide exchange factor ECT2 interacts with the polarity protein complex Par6/Par3/protein kinase Czeta (PKCzeta) and regulates PKCzeta activity. Mol. Cell. Biol. *24*, 6665–6675.

Ma, A., Richardson, A., Schaefer, E. M., and Parsons, J. T. (2001). Serine phosphorylation of focal adhesion kinase in interphase and mitosis: a possible role in modulating binding to p130(Cas). Mol. Biol. Cell *12*, 1–12.

Maddox, A. S., and Burridge, K. (2003). RhoA is required for cortical retraction and rigidity during mitotic cell rounding. J. Cell Biol. *160*, 255–265.

Maddox, A. S., and Oegema, K. (2003). Closing the GAP: a role for a RhoA GAP in cytokinesis. Mol. Cell *11*, 846–848.

Manes, T., Zheng, D. Q., Tognin, S., Woodard, A. S., Marchisio, P. C., and Languino, L. R. (2003). $\alpha(v)\beta 3$ Integrin expression up-regulates cdc2, which modulates cell migration. J. Cell Biol. *161*, 817–826.

Marumoto, T., Zhang, D., and Saya, H. (2005). Aurora-A–a guardian of poles. Nat. Rev. Cancer *5*, 42–50.

Matuliene, J., and Kuriyama, R. (2002). Kinesin-like protein CHO1 is required for the formation of midbody matrix and the completion of cytokinesis in mammalian cells. Mol. Biol. Cell *13*, 1832–1845.

Maupin, P., and Pollard, T. D. (1986). Arrangement of actin filaments and myosin-like filaments in the contractile ring and of actin-like filaments in the mitotic spindle of dividing HeLa cells. J. Ultrastruct. Mol. Struct. Res. *94*, 92–103.

Minoshima, Y., *et al*. (2003). Phosphorylation by Aurora B Converts MgcRacGAP to a RhoGAP during Cytokinesis. Dev. Cell *4*, 549–560.

Nagasaki, A., De Hostos, E. L., and Uyeda, T. Q. (2002). Genetic and morphological evidence for two parallel pathways of cell-cycle-coupled cytokinesis in *Dictyostelium*. J. Cell Sci. *115*, 2241–2251.

Nakamoto, T., Sakai, R., Ozawa, K., Yazaki, Y., and Hirai, H. (1996). Direct binding of the C-terminal region of p130-Cas to SH2 and SH3 domains of Src kinase. J. Biol. Chem. *271*, 8959–8965.

O'Keefe, L., Somers, W. G., Harley, A., and Saint, R. (2001). The pebble GTP exchange factor and the control of cytokinesis. Cell Struct. Funct. *26*, 619–626.

O'Neill, G. M., Fashena, S. J., and Golemis, E. A. (2000). Integrin signaling: a new Cas(t) of characters enters the stage. Trends Cell Biol. *10*, 111–119.

O'Neill, G. M., and Golemis, E. A. (2001). Proteolysis of the docking protein HEF1 and implications for focal adhesion dynamics. Mol. Cell. Biol. *21*, 5094–5108.

Orly, J., and Sato, G. (1979). Fibronectin mediates cytokinesis and growth of rat follicular cells in serum-free medium. Cell *17*, 295–305.

Polte, T. R., and Hanks, S. K. (1995). Interaction between focal adhesion kinase and Crk-associated tyrosine kinase substrate p130Cas. Proc. Nat. Acad. Sci. USA *92*, 10678–10682.

Prokopenko, S. N., Brumby, A., O'Keefe, L., Prior, L., He, Y., Saint, R., and Bellen, H. J. (1999). A putative exchange factor for Rho1 GTPase is required for initiation of cytokinesis in *Drosophila*. Genes Dev. *13*, 2301–2314.

Prokopenko, S. N., Saint, R., and Bellen, H. J. (2000). Tissue distribution of PEBBLE RNA and pebble protein during *Drosophila* embryonic development. Mech. Dev. *90*, 269–273.

Pugacheva, E. N., and Golemis, E. A. (2005). The focal adhesion scaffolding protein HEF1 regulates activation of the Aurora-A and Nek2 kinases at the centrosome. Nat. Cell Biol. *7*, 937–946.

Raff, J. W., Jeffers, K., and Huang, J. Y. (2002). The roles of Fzy/Cdc20 and Fzr/Cdh1 in regulating the destruction of cyclin B in space and time. J. Cell Biol. *157*, 1139–1149.

Ren, X. D., Kiosses, W. B., Sieg, D. J., Otey, C. A., Schlaepfer, D. D., and Schwartz, M. A. (2000). Focal adhesion kinase suppresses Rho activity to promote focal adhesion turnover. J. Cell Sci. *113*, 3673–3678.

Ridley, A. J. (2001). Rho GTPases and cell migration. J. Cell Sci. *114*, 2713–2722.

Ridley, A. J., and Hall, A. (1992). The small GTP-binding protein rho regulates the assembly of focal adhesions and actin stress fibers in response to growth factors. Cell *70*, 389–399.

Saito, S., *et al*. (2004). Deregulation and mislocalization of the cytokinesis regulator ECT2 activate the Rho signaling pathways leading to malignant transformation. J. Biol. Chem. *279*, 7169–7179.

Saito, S., Tatsumoto, T., Lorenzi, M. V., Chedid, M., Kapoor, V., Sakata, H., Rubin, J., and Miki, T. (2003). Rho exchange factor ECT2 is induced by growth factors and regulates cytokinesis through the N-terminal cell cycle regulator-related domains. J. Cell. Biochem. *90*, 819–836.

Sakai, R., Iwamatsu, A., Hirano, N., Ogawa, S., Tanaka, T., Mano, H., Yazaki, Y., and Hirai, H. (1994). A novel signaling molecule, p130, forms stable complexes in vivo with v-Crk and v-Src in a tyrosine phosphorylation-dependent manner. EMBO J. *13*, 3748–3756.

Sakai, R., Nakamoto, T., Ozawa, K., Aizawa, S., and Hirai, H. (1997). Characterization of the kinase activity essential for tyrosine phosphorylation of p130Cas in fibroblasts. Oncogene *14*, 1419–1426.

Savoian, M. S., Earnshaw, W. C., Khodjakov, A., and Rieder, C. L. (1999). Cleavage furrows formed between centrosomes lacking an intervening spindle and chromosomes contain microtubule bundles, INCENP, and CHO1 but not CENP-E. Mol. Biol. Cell *10*, 297–311.

Schlaepfer, D. D., Hauck, C. R., and Sieg, D. J. (1999). Signaling through focal adhesion kinase. Prog. Biophys. Mol. Biol. *71*, 435–478.

Schwartz, M. A. (1997). Integrins, oncogenes, and anchorage independence. J. Cell Biol. *139*, 575–578.

Schwartz, M. A., and Shattil, S. J. (2000). Signaling networks linking integrins and rho family GTPases. Trends Biochem. Sci. *25*, 388–391.

Sinnett-Smith, J., Lunn, J. A., Leopoldt, D., and Rozengurt, E. (2001). Y-27632, an inhibitor of Rho-associated kinases, prevents tyrosine phosphorylation of focal adhesion kinase and paxillin induced by bombesin: dissociation from tyrosine phosphorylation of p130(CAS). Exp. Cell Res. *266*, 292–302.

Solski, P. A., Wilder, R. S., Rossman, K. L., Sondek, J., Cox, A. D., Campbell, S. L., and Der, C. J. (2004). Requirement for C-terminal sequences in regulation of Ect2 guanine nucleotide exchange specificity and transformation. J. Biol. Chem. *279*, 25226–25233.

Tatsumoto, T., Sakata, H., Dasso, M., and Miki, T. (2003). Potential roles of the nucleotide exchange factor ECT2 and Cdc42 GTPase in spindle assembly in *Xenopus* egg cell-free extracts. J. Cell. Biochem. *90*, 892–900.

Tatsumoto, T., Xie, X., Blumenthal, R., Okamoto, I., and Miki, T. (1999). Human ECT2 is an exchange factor for Rho GTPases, phosphorylated in G2/M phases, and involved in cytokinesis. J. Cell Biol. *147*, 921–928.

Van Aelst, L., and D'Souza-Schorey, C. (1997). Rho GTPases and signaling networks. Genes Dev. *11*, 2295–2322.

van Seventer, G. A., Salman, H. J., Law, S. F., O'Neill, G. M., Mullen, M. M., Franz, A. A., Kanner, S. B., Golemis, E. A., and van Seventer, J. M. (2001). Focal adhesion kinase regulates beta1 integrin dependent migration through an HEF1 effector pathway. Eur. J. Immunol. *31*, 1417–1427.

Vuori, K., Hirai, H., Aizawa, S., and Ruoslahti, E. (1996). Induction of p130Cas signaling complex formation upon integrin-mediated cell adhesion: a role for Src family kinases. Mol. Cell. Biol. *16*, 2606–2613.

Yamaguchi, R., Mazaki, Y., Hirota, K., Hashimoto, S., and Sabe, H. (1997). Mitosis specific serine phosphorylation and downregulation of one of the focal adhesion protein, paxillin. Oncogene *15*, 1753–1761.

Yamakita, Y., Totsukawa, G., Yamashiro, S., Fry, D., Zhang, X., Hanks, S. K., and Matsumura, F. (1999). Dissociation of FAK/p130(CAS)/c-Src complex during mitosis: role of mitosis-specific serine phosphorylation of FAK. J. Cell Biol. *144*, 315–324.

Yi, J., Kloeker, S., Jensen, C. C., Bockholt, S., Honda, H., Hirai, H., and Beckerle, M. C. (2002). Members of the zyxin family of LIM proteins interact with members of the p130cas family of signal transducers. J. Biol. Chem. *277*, 9580–9589.

Yoshizaki, H., Ohba, Y., Parrini, M. C., Dulyaninova, N. G., Bresnick, A. R., Mochizuki, N., and Matsuda, M. (2004). Cell type-specific regulation of RhoA activity during cytokinesis. J. Biol. Chem. *279*, 44756–44762.